



**HAL**  
open science

## A Combined Cycle Gas Turbine Model for Heat and Power Dispatch Subject to Grid Constraints

Rémy Rigo-Mariani, Chuan Zhang, Alessandro Romagnoli, Markus Kraft,  
Keck Voon Ling, Jan Maciejowski

► **To cite this version:**

Rémy Rigo-Mariani, Chuan Zhang, Alessandro Romagnoli, Markus Kraft, Keck Voon Ling, et al.. A Combined Cycle Gas Turbine Model for Heat and Power Dispatch Subject to Grid Constraints. IEEE Transactions on Sustainable Computing, 2019, 11 (1), pp.448-456. 10.1109/TSTE.2019.2894793 . hal-03016628

**HAL Id: hal-03016628**

**<https://hal.science/hal-03016628>**

Submitted on 20 Nov 2020

**HAL** is a multi-disciplinary open access archive for the deposit and dissemination of scientific research documents, whether they are published or not. The documents may come from teaching and research institutions in France or abroad, or from public or private research centers.

L'archive ouverte pluridisciplinaire **HAL**, est destinée au dépôt et à la diffusion de documents scientifiques de niveau recherche, publiés ou non, émanant des établissements d'enseignement et de recherche français ou étrangers, des laboratoires publics ou privés.

# A Combined Cycle Gas Turbine Model for Heat and Power Dispatch Subject to Grid Constraints

Rémy Rigo-Mariani, Chuan Zhang, Alessandro Romagnoli, Markus Kraft, Keck Voon Ling, Jan Maciejowski

Cambridge Centre for Advanced Research and Education in Singapore Ltd, 1 Create Way, 138602, Singapore  
Nanyang Technological University, 50 Nanyang Ave, 639798 Singapore

**Abstract**—This paper investigates an optimal scheduling method for the operation of combined cycle gas turbines (CCGT). The objective is to minimize the CO<sub>2</sub> emissions while supplying both electrical and thermal loads. The paper adopts a detailed model of the units in order to relate the heat and power outputs. The grid constraints as well as system losses are considered for both the electrical and thermal systems. Finally, the optimal power dispatch lies on the hybridization of a Mixed Integer Linear Programming (MILP) scheduling with a greedy search method. Different sets of simulations are run for a small 5-bus test case and a larger model of Jurong Island in Singapore. Several load levels are considered for the heat demand and the impact of the steam pipe capacities is highlighted.

**Index Terms**—Combined Cycle, cogeneration, security constrained unit commitment, MILP.

## I. NOMENCLATURE

### Sets:

$i \in I$	set of units
$t \in T$	set of time steps
$r \in R$	set of possible values for power/heat ratio
$s \in S$	special order set for GT output (2 blocks)
$k \in K$	set of breakpoints over $S$ (3 breakpoints)
$c \in C$	special order set for carbon cost (2 blocks)
$b \in B$	set of buses
$l^e \in L^E$	set of power (electricity) lines
$l^h \in L^H$	set of thermal (heat) lines

### Variables :

$\alpha_{i,t}^{ph}$	power/heat ratio of unit $i$ at time $t$
$\alpha_{i,t,r}^{ph,b}$	power/heat ratio $r$ of unit $i$ at time $t$ $\{0,1\}$
$u_{i,t}$	on/off status of unit $i$ at time $t$ $\{0,1\}$
$v_{i,t}$	unit $i$ start-up at time $t$ $\{0,1\}$
$w_{i,t,r,s}^e, w_{i,t,r,s}^h$	unit $i$ with ratio $r$ in block $s$ at time $t$ $\{0,1\}$
$\beta_{i,t,r,k}^e, \beta_{i,t,r,k}^h$	weight of point $k$ unit $i$ with ratio $r$ at time $t$
$P_{i,t}^{gt}$	gas turbine output of unit $i$ at time $t$
$P_{i,t}^e, P_{i,t}^h$	electrical/heat outputs of unit $i$ at time $t$
$P_{i,t,c}^{gt}$	GT unit $i$ at time $t$ in block $c$ for CO <sub>2</sub> cost
$P_{b,t}^{bl}, P_{b,t}^{dp}$	Boiler/damp heat at bus $b$ at time $t$
$P_t^{bl}, P_t^{dp}$	boiler output and damp heat load at time $t$
$F_{l,t}^{e+}, F_{l,t}^{e-}$	positive/negative flows in line $l^e$ at time $t$
$F_{l,t}^h$	flow in line $l^h$ at time $t$

### Parameters:

$G_{i,r,k}^{gt,e}, G_{i,r,k}^{gt,h}$	GT breakpoints $k$ of unit $i$ with ratio $r$
$G_{i,r,k}^e, G_{i,r,k}^h$	power/heat breakpoints $k$ of unit $i$ at ratio $r$
$P_i^{gt,m}, P_i^{gt-M}$	min/max output of GT in unit $i$
$P_t^{L-e}, P_t^{L-h}$	total power/heat load at time $t$
$P_{b,t}^{L-e}, P_{b,t}^{L-h}$	power/heat load at bus $b$ at time $t$
$A_{i,c}$	slope for carbon cost of unit $i$ in block $c$
$C_{0b}, SU_i$	base cost and start-up cost of unit $i$
$P_{i,c}^{gt,M}$	upper bound of block $c$ for GT of unit $i$
$A^{bl}$	boiler CO <sub>2</sub> emissions
$F_{l^e}^{e,M}$	max power flow in power line $l^e$
$F_{l^h}^{h,des}$	design capacity of thermal line $l^h$
$\delta_{l^e}^e, \delta_{l^h}^h$	power/heat lines loss coefficients
$\theta$	range of heat flow in steam pipes (in %)
$SF_{L^E B}$	$L^E \times B$ matrix with generation shift factors
$M_{BL^E}^c$	$B \times L^E$ matrix that maps the power network
$M_{BI}$	$B \times I$ matrix that maps the units in the grid
$M_{BL^H}^{h+}, M_{BL^H}^{h-}$	$B \times L^H$ matrixes that map the heat network

## II. INTRODUCTION

Combined heat and power (CHP) cogeneration systems are widely used assets for both residential and industrial applications due to their high global efficiency as well as economic and environmental benefits. Operation of such units has been extensively addressed in the literature, mainly targeting total revenue maximization and/or emissions minimization. Optimal scheduling problems are commonly investigated to supply both heat and electrical loads in the presence of storage devices [1]-[2] or renewable energy sources [3]. Another class of related studies refers to planning problems with the sizing of CHP generators [3] or the design of waste heat recovery networks [5]. Most of those optimization frameworks assume coarse models for the generators. Usually, an operating region for the units power and heat outputs is assumed resulting in linear constraints for the scheduling problems [1]-[2]-[5]. Another shortcoming often encountered in the literature lies in the lack of representation of both thermal and electrical networks. Recent studies have pointed out that coupling of thermal and electricity grids in the cogeneration system would bring additional flexibility, as well as complexity, to the system operation regime, making the optimization of such cogeneration systems difficult [5]-[7]. This paper aims at

addressing the two aforementioned points. First, a realistic model of combined cycle gas turbine (CCGT) is considered. In particular, that representation taken from previous work [7] estimates the CO<sub>2</sub> emissions of the units all along their operating range, by the computation of the chemical reaction within the combustion chamber. Secondly, the optimal scheduling of the units takes both power and heat network constraints into account, as well as the losses within the cables and the pipes. The last contribution of the paper lies in the hybridization of a Mixed Integer Linear Programming (MILP) scheduling with a greedy search method. The objective is to avoid prohibitive computational times when large numbers of units are considered. Also note that with recent developments in cyber-physical systems for energy system management (e.g. J-Park Simulator [9]), the model proposed in the paper could be integrated with real data from smart meters to unleash the potential of real-time control of CHP systems. The rest of the paper is organized as follows. Section III presents the model for the CCGT as well as the MILP formulation that allows one to compute the power/heat outputs. Section IV integrates that model in an optimal dispatch problem whose objective is the minimization of the CO<sub>2</sub> emissions over a representative day (no cost of generation are considered here). Then, Section V introduces the representation of the power grid and heat network. Finally, sets of simulations are run for a small 5-bus test case and a model of the Jurong Island in Singapore.

### III. CCGT MODEL

#### A. CCGT Operation for Heat and Power Generation

The work presented in this paper has been done in the context of the C4T project whose objective is carbon reduction in industrial/chemical activities. Jurong Island in Singapore is considered as a case study. That island hosts half the power generation capacity in Singapore. Most of the production is consumed on site by heavy customers (oil refineries and chemical facilities) while the surplus is exported to the Singaporean mainland. Previous work focused on system modeling with specific attention given to the representation of the combined CCGT on site [7]. The operation of such units relies on the combination of two thermodynamic cycles. In the top Brayton cycle, the input air-mass flow ( $m_a$  in kg/s) at ambient conditions is compressed by a ratio  $r_c$  before entering the combustion chamber and being heated to the turbine inlet temperature ( $TIT$  in °C). Power is then produced by the expansion of the hot gases in the gas turbine (GT) whose shaft is connected to the generator. In the bottom Rankine cycle, the hot gases at the turbine-exhaust temperature ( $TET$  in °C) are used in a heat recovery steam generator (HRSG) to produce superheated steam at high temperature for a steam turbine (ST) with an efficiency  $\eta_{st}$ . Thus, the combined-cycle (CC) units allow exploitation of the available heat in the exhaust gas of the gas turbine and enhancement of the power generation efficiency from 40% ( $\eta_{gt}$ ) to 60% ( $\eta_{cc}$ ) [10]. A conventional way to operate these units consists of the control of the inlet guide vane (IGV) of the compressor. The IGV is controlled up to a 30% air-flow reduction with a constant  $TET$  followed by a control of the maximum air flow [11] (Fig. 1a).

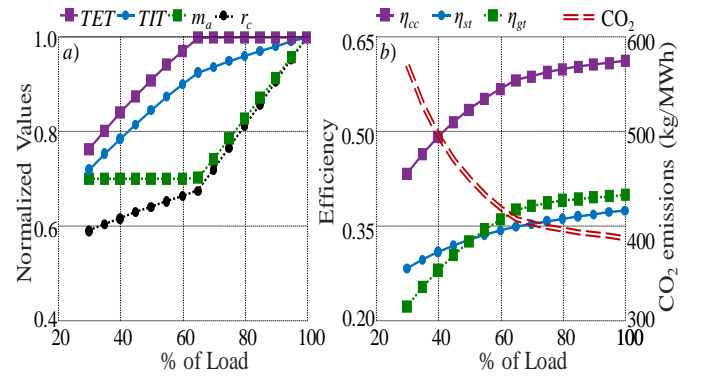


Fig. 1: CCGT normal operation - a) operating variables - b) performances [7]

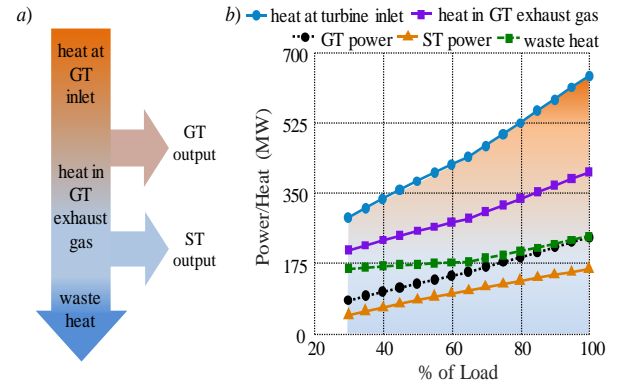


Fig. 2: Power and Heat - a) power sharing - b) Operating performances [7]

A model was developed in [7] to estimate the performance and the CO<sub>2</sub> emissions of different technologies over their whole operating range (typically from 30 % to 100 % of the nominal electrical output). Fig. 1b displays a sample of the obtained results, with increased efficiencies at the designed operating point (i.e. 100 %). The developed model allow one to identify the share between heat and power in the units all along the two cycles (Fig. 2a) and for different operating points (Fig. 2b). Note that the estimated amount of heat in the GT exhaust gas is significant. This justifies the use of a combined cycle to enhance the efficiency of the energy generation, with an overall electrical output computed as the sum of both GT and ST powers.

The previous work only considered the electrical output and performed an environmental unit commitment (UC) in order to supply a given power load profile over a representative day while minimizing the corresponding CO<sub>2</sub> emissions. In this paper the CCGT units are considered as cogeneration assets with the ability to provide both heat and power, with the waste heat transferred into a thermal network. In addition, the amount of transferred heat is adjustable by varying the proportion of GT exhaust gases dedicated to the power generation at the ST stage. A power/heat ratio  $\alpha_{i,t}^{ph}$  (between 0 and 1) is then introduced considering the operation of unit  $i$  at time  $t$ . Thus for a given power output of the gas turbine  $P_{i,t}^{gt}$  (in MW) different operating conditions can be computed and correspond to distinct values for the overall electrical and heat outputs of the unit - respectively  $P_{i,t}^e$  and  $P_{i,t}^h$  in MW.

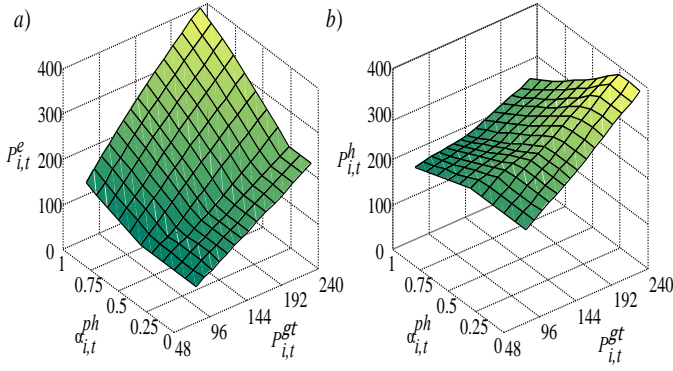


Fig. 3: CCGT power/heat operation – a) power output – b) heat output

Fig. 3 shows the results obtained while running the model for a 400 MW CCGT unit with a 240 MW GT and a 160 MW ST. As expected, both electrical and heat outputs increase with the operating point of the gas turbine. A case with  $\alpha_{i,t}^{ph}=1$  corresponds to the nominal operation described in Fig. 1 with the maximum electrical output reached for a gas turbine operating at 100 % (Fig. 3a). That power generation significantly decreases when the power/heat ratio becomes lower, leading to more waste heat (Fig. 3b). In such a case the priority is given to the thermal generation. Only a small part of the nominal waste heat coming from the GT is available. Consequently, the output of the steam turbine is assumed to be null and the CCGT power only corresponds to the gas turbine output.

### B. MILP Formulation for CCGT Operation

As will be presented in the next section, the objective of the proposed heat and power dispatch is to supply both thermal and electrical loads with minimal emissions of CO<sub>2</sub>. A MILP approach is considered in order to ensure reasonable computational times, as is commonly done in the literature when the commitment of a large number of units with temporal constraints is investigated **Erreur! Source du renvoi introuvable.** [5]. The gas turbine output and the power/heat ratio of the units are considered as controls. Additional variables and constraints need to be introduced in order to model both electrical and thermal outputs for a given set of controls. In other words, the concern here is to represent the surfaces plotted in Fig. 3 in the MILP formulation. Thus linearization methods for functions of two variables are considered [12]. Traditional triangular or rectangular approaches offer the best performance but require a great number of variables (continuous and binary) that could lead to prohibitive computational times. For the sake of simplicity, a 1D method is considered here. With functions of two variables, the idea is to keep one continuous variable ( $P_{i,t}^{gt}$  in this case) while the other is discretized. Thus  $\alpha_{i,t}^{ph}$  is substituted by a binary variable  $\alpha_{i,t,r}^{ph,b}$  with  $r \in R$  the set of possible values for the power/heat ratio. Arbitrarily, a set of eleven different values is chosen and corresponds to the discretization along  $\alpha_{i,t}^{ph}$  displayed in Fig. 3 (i.e.  $r=1$  for  $\alpha_{i,t}^{ph}=0$  and  $r=11$  for  $\alpha_{i,t}^{ph}=1$ ). Thus  $\alpha_{i,t,r}^{ph,b}=1$  allows one to identify at which ratio  $r$  a unit  $i$  is operated at time  $t$ . The electrical and heat outputs are then computed by defining a special ordered set over  $P_{i,t}^{gt}$  [12] with a two-block piecewise linearization (set  $S$ ). The following equations describe the set of variables and constraints to model

the electrical power output (subscript  $e$ ) - the thermal components (subscript  $h$ ) are treated similarly. First, an additional binary variable  $w_{i,t,r,s}^e$  is introduced and is equal to 1 if unit  $i$  is operated with ratio  $r$  in block  $s$  at time  $t$ . Constraints (1) ensure that only one operating block is identified provided that the unit is on at time  $t$  (i.e.  $u_{i,t}=1$ ). A continuous variable  $\beta_{i,t,r,k}^e$  represents the weight coefficients attached to the  $k$  breakpoints that border each block  $s$  ( $K=S+1$ ). With constraints in (2), only the weights for the two breakpoints around the operating block are non-null.  $s_{x-1}$  and  $s_{x+1}$  denote the two segments around a breakpoint  $k_x$  with  $w_{i,t,r,s_x}^e = 0$  for the “extreme” breakpoints (i.e.  $x=0$  and  $x=K+1$ ). As the sum of those weights is equal to one by (3), the GT power is computed following (4) with the breakpoints  $G_{i,t,r,k}^{gt,e}$  entered as parameters. Fig. 4 shows an example for the GT power computation of a unit operating in a specific block  $s_l$  for a given heat/power ratio. Constraints (5) are introduced over the whole set  $R$  in order to compute the electrical output corresponding to the operating power/heat ratio and the calculated  $P_{i,t}^{gt,e}$ . With an appropriate “Big  $M$ ” value (typically  $10^6$ ) only the constraints referring to  $\alpha_{i,t,r}^{ph,b}=1$  will be active [12]. Equation (6) ensures that only a single value of the power/heat ratio is considered for every unit at each time step.  $P_{i,t}^{gt,e}$  is then computed similarly to the GT output with the weight coefficients for the breakpoints  $G_{i,t,r,k}^{gt,e}$  entered as parameters.

$$\sum_{s \in S} w_{i,t,r,s}^e = u_{i,t} \quad (1)$$

$$\begin{cases} \beta_{i,t,r,k}^e \geq 0 \\ \beta_{i,t,r,k_x}^e \leq w_{i,t,r,s_{x-1}}^e + w_{i,t,r,s_{x+1}}^e \end{cases} \quad (2)$$

$$\sum_{k \in K} \beta_{i,t,r,k}^e = u_{i,t} \quad (3)$$

$$P_{i,t}^{gt} = \sum_{k \in K} \beta_{i,t,r,k}^e \times G_{i,r,k}^{gt,e} \quad (4)$$

$$\begin{cases} P_{i,t}^e \leq \sum_{k \in K} \beta_{i,t,r,k}^e \times G_{i,r,k}^e + M \times (1 - \alpha_{i,t,r}^{ph,b}) \\ P_{i,t}^e \geq \sum_{k \in K} \beta_{i,t,r,k}^e \times G_{i,r,k}^e - M \times (1 - \alpha_{i,t,r}^{ph,b}) \end{cases} \quad (5)$$

$$\sum_{r \in R} \alpha_{i,t,r}^{ph,b} = 1 \quad (6)$$

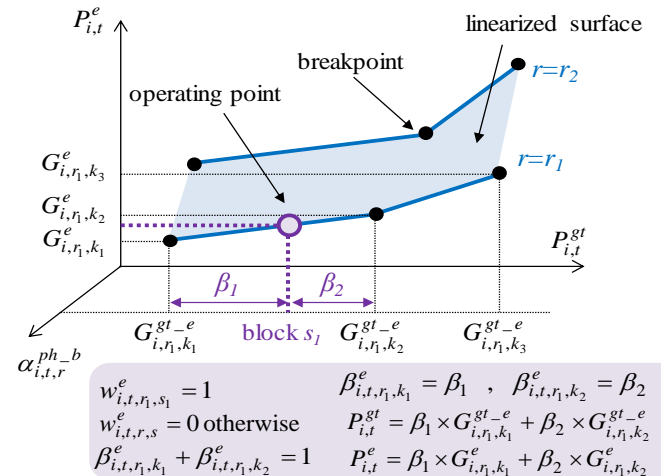


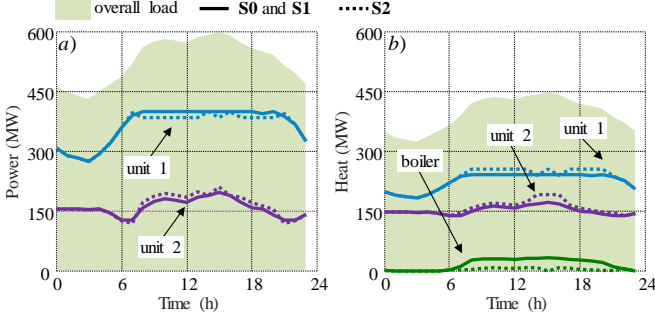
Fig. 4: Example of unit  $i$  operating in block  $s_1$  with ratio  $r_1$  at time  $t$ 

Fig. 5: Obtained results with two units – a) power dispatch – b) heat dispatch

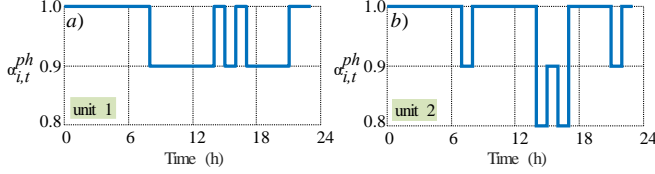


Fig. 6: Power/heat ratio – a) unit 1 – b) unit 2

#### IV. HEAT AND POWER DISPATCH

##### A. Classical Unit Commitment MILP Formulation

The model developed in the previous section is now included in an environmental unit commitment for both heat and power dispatch. As already mentioned, the objective is to supply power ( $P_t^{L,e}$ ) and heat ( $P_t^{L,h}$ ) load profiles with a set of different CCGT units and with minimal CO<sub>2</sub> emissions. A classical two-block ( $c \in C$ ) linearization of the carbon cost is considered [13] regarding the GT output. The objective over the time horizon is computed following (7) with an hourly time step. That function depends on the operating block for the GT of unit  $i$  at time ( $p_{i,t,c}^{gt}$ ) and considering the corresponding block slope  $A_{i,c}$ , the base cost  $C_{0i}$  and the start-up cost  $SU_i$  – with  $v_{i,t}=1$  when unit  $i$  starts up at time  $t$ . An additional boiler with CO<sub>2</sub> coefficient  $A_{bl}$  (in kg/MWh [14]-[15]) is considered to supply the heat load if the units' heat outputs are not enough – surplus denoted as  $P_t^{bl}$  (in MW). In order to ensure the convergence a thermal damp load  $P_t^{dp}$  also needs to be introduced if the units generate too much heat. Thus, implicitly priority is given to the supply of the electrical load in the current implementation. Note that both  $P_t^{bl}$  and  $P_t^{dp}$  are unbounded positive variables.

$$\min_{u_{i,t}, v_{i,t}, p_{i,t,c}^{gt}} \sum_{t \in T} \sum_{i \in I} \left( C_{0i} \times u_{i,t} + \sum_{c \in C} A_{i,c} \times p_{i,t,c}^{gt} + SU_i \times v_{i,t} \right) + A^{bl} \times P_t^{bl} \quad (7)$$

$$u_{i,t} \times P_i^{gt-m} \leq P_{i,t}^{gt} \leq u_{i,t} \times P_i^{gt-M} \quad (8)$$

$$P_{g,t} = u_{i,t} \times P_i^{gt-m} + \sum_{c \in C} P_{i,t,c}^{gt} \quad (9)$$

$$0 \leq P_{i,t,c}^{gt} \leq P_{i,c}^{gt-M} \quad (10)$$

$$v_{i,t} \geq u_{i,t} - u_{i,t-1} \quad (11)$$

$$\sum_{i \in I} P_{i,t}^e = P_t^{L-e} \quad (12)$$

$$\sum_{i \in I} P_{i,t}^h + P_t^{bl} - P_t^{dp} = P_t^{L-h} \quad (13)$$

Constraints (8)-(10) ensure that all the units properly work in the linear block identified in the objective function. Typical operating constraints in UC refer to minimum up and down times for the units, ramping limits or shut down cost [16]. For clarity they do not appear here and only the logical constraints (11) are considered. Finally, (12) and (13) allow one to fulfill both power and heat balances at each time step. The problem is formulated in MATLAB using YALMIP [17] and solved using CPLEX 12.7.1 (16 threads in parallel, 16 GB RAM, 3.2 GHz processor).

##### B. Results for a Two Units Dispatch

Initially, simulations are performed for a dispatch with two units. Unit 1 is a high efficiency 400 MW CCGT with specific CO<sub>2</sub> emissions of 390 kg/MWh (at its nominal point). Unit 2 has higher specific CO<sub>2</sub> emissions with 450 kg/MWh (at its nominal point) for a maximum capacity of 250 MW. More information on the considered technologies and the modeling aspects can be found in [7]. Three different strategies are investigated. In **S0** the two units are optimally dispatched to feed the electrical load while the heat demand is supplied by the boiler. The same dispatch strategy is considered in **S1** but the CCGT waste heat is injected into a thermal network. The boiler and damp load allow to adjust the amount of heat provided. Finally, **S2** denotes the power/heat ratio management previously described. For **S0** and **S1** the optimal results correspond to the cleaner unit working at its maximum electrical output while Unit 2 provides the surplus of energy during the peak period (Fig. 5a). The ability to control the power/heat ratio tends to lower the power output of Unit 1 in order to favor its heat generation (Fig. 5b). At the same time the operating point of Unit 2 (in terms of GT power) is increased with higher power and heat outputs in **S2**. Note that with a significant electrical load compared to the heat demand, the power/heat ratio cannot reach values below 0.8 to ensure convergence (Fig. 6). In **S2** more waste heat from the CCGT units is transferred to the thermal network which lowers the need for the additional boiler. Consequently, the overall amount of CO<sub>2</sub> generated while supplying heat and power is reduced. – from 5214 tons to 5195 tons in the previous simulations with specific emissions of 300 kg/MWh for the boiler. Obviously, the CO<sub>2</sub> reduction becomes more significant with 'dirtier' boilers as shown in Table I. The same observation can be made when the level of the heat load increases regarding the power demand with  $\delta = P_t^{L-h}/P_t^{L-e}$  (simulation in Fig. 5 corresponds to  $\delta = 75\%$ ). For higher heat load levels the improvement provided by the management of the power/heat ratios is more significant regardless of the boiler emissions (Fig. 7).

TABLE I  
CO<sub>2</sub> emissions for different  $A^{bl}$

$A^{bl}$ (kg/MWh)	<b>S0</b>	<b>S1</b>	<b>S2</b>
300	7921	5214	5195
500	9812	5286	5201
700	11704	5337	5201

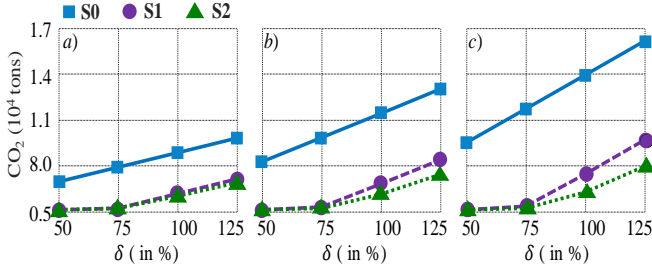


Fig. 7: CO<sub>2</sub> Vs the heat load level – a)  $A^{bl}=300$  - b)  $A^{bl}=500$  - c)  $A^{bl}=700$

### C. Constant Power/Heat Ratios

The computational time for the previous simulation with two units was very low at around 18 s. However, preliminary tests with five units showed no convergence after more than four hours of computation. Indeed, although the solver can easily handle the 5376 binary variables in the two-CCGT problem, this is not the case with five units (13440 binary variables) or thirteen units (34944 binary variables) as in the Jurong Island model [7]. The complexity of the developed model mainly lies in the introduction of multiple possible values for  $\alpha_{i,t,r}^{ph-b}$ . A first simplification could consist of reducing the size of the set  $R$  with fewer values for the power/heat ratios (e.g.  $\{0, 0.3, 0.6, 1\}$ ). Instead, a constant ratio over the time horizon is considered here. The set  $R$  remains the same as previously (i.e. 11 possible values) and constraint (6) is rewritten as follows with  $r_i^{ref}$  the constant power/heat ratio of unit  $i$  over the day (with  $r$  an integer in  $\{1, \dots, 11\}$ ).

$$\begin{cases} \alpha_{i,t,r}^{ph-b} = 1 & \text{if } r = r_i^{ref} \quad \forall t \in T \\ \alpha_{i,t,r}^{ph-b} = 0 & \text{otherwise} \end{cases} \quad (14)$$

A new set of simulations is performed while varying the references for the power/heat ratios of the two units. Also, the impact of the power load level is investigated for three cases: low (**L** at 50%), middle (**M** at 75%) and high (**H** at 100%). The heat load profile remains the same as previously and  $A^{bl} = 500$  kg/MWh. An exhaustive search is performed to find the best set of constant ratios ( $r_1^{ref}$  and  $r_2^{ref}$ ) that minimizes the emissions. That approach is denoted as **S3**. As already observed in the previous subsection, results obtained with **S2** are better than in a case where the power/heat ratio of the unit remains at one (i.e. **S1**) (Table II). The improvements increase when the heat load is more significant compared to the electrical demand (i.e. moving from **H** to **L** here). The strategy **S3** with constant ratios displays intermediate results that become closer to the performances of **S2** with lower power loads. Fig. 8 plots the results obtained while varying ratios  $r_1^{ref}$  and  $r_2^{ref}$  for the different power load levels. For higher electrical demands the dispatch strategy cannot converge with low ratios. In such cases the combined power output of the two units is not enough to supply the load (Fig. 8b,c). Considering case **L**, the convergence is obtained whatever the chosen reference ratios are (Fig. 8a). Each of the plotted surfaces displays a global minimum that corresponds to the optimal set of power/heat ratios with the lowest CO<sub>2</sub> emissions.

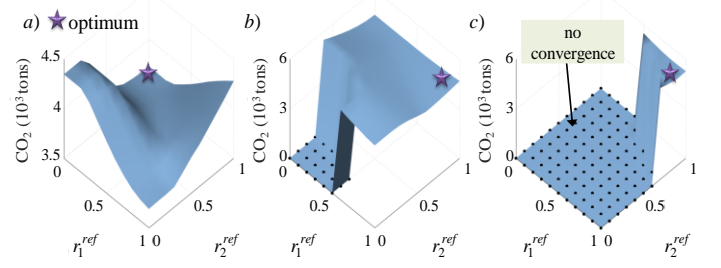


Fig. 8: Obtained results with **S3** – a) level **L** – b) level **M** – c) level **H**

TABLE II  
CO<sub>2</sub> emissions for different power load levels

Power load level	<b>S1</b>	<b>S2</b>	<b>S3</b>
<b>L</b>	4282	3665	3693
<b>M</b>	4684	4411	4476
<b>H</b>	5286	5201	5243

The exhaustive search performed by **S3** is possible in a case with two units and only requires 30 min with 121 different sets of ratios estimated (i.e.  $11^2$ ). However, computational times might become prohibitive when more generators are considered (e.g.  $11^{13}$  possible sets for the Jurong Island model). To overcome that difficulty a greedy search method is implemented and the MILP dispatch is successively run for different sets of power/heat ratios. The idea of the method is to iteratively decrease the ratios of the units until no improvement is possible in the objective ( $obj^*$ ). At each iteration the method identifies the unit whose power/heat ratio should be decreased in order to reduce the emissions as much as possible (Table III). That is done by independently decreasing the ratio of each unit  $i$  and computing the corresponding emissions ( $obj_i$ ). For the three different power load levels (i.e. low **L**, medium **M** and high **H**) the developed algorithm returns the same solution as the exhaustive search **S3**. However, it is obvious that the greedy approach cannot guarantee a global optimum in every case. The main advantage lies in a limited computational time with a maximum number of evaluations (i.e. runs of the MILP dispatch) directly linked to the number of units and the size of the set  $R$  – maximum of  $R \times I \times I$  evaluations.

TABLE III  
Hybrid Greedy/MILP dispatch

Outputs	Return $r_i^{ref}$ for $i \in I$
<b>Set</b> $r_i^{ref} = 1$ and $obj_i = 0$ for $i \in I$	
<b>Run</b> MILP dispatch and compute $obj^*$	
<b>While</b> $\min(obj_i) < obj^*$	
<b>For</b> $i \in I$	
<b>If</b> $r_i^{ref} > 1$	
$r_i^{ref} \leftarrow r_i^{ref} - 1$	
<b>Run</b> MILP dispatch and compute $obj_i$	
<b>If</b> no convergence, $obj_i = \infty$ , <b>End If</b>	
$r_i^{ref} \leftarrow r_i^{ref} + 1$	
<b>Else</b> $obj_i = \infty$	
<b>End If</b>	
<b>End For</b>	
<b>If</b> $\min(obj_i) < obj^*$	
$obj^* \leftarrow \min(obj_i)$	
$r_i^{ref} \leftarrow r_i^{ref} - 1$ for $i$ corresponding to $\min(obj_i)$	
<b>End If</b>	
<b>End While</b>	

## V. SECURITY CONSTRAINED DISPATCH

### A. Introduction of Losses and Grid Constraints.

The previous subsection introduced an optimal power/heat dispatch in the presence of cogeneration units. A security constrained unit commitment is now considered with the inclusion of models for power and thermal networks. The objective is to take account of possible constraints regarding the flows within electrical cables and steam pipes.

#### 1) Electrical Grid Model

For the power system a traditional DC power flow model is considered with the computation of Shift Factors ( $\mathbf{SF}_{L^E B}$ ) [18]. Then the power flow within a line  $l^e$  at time  $t$  is computed by considering both positive and negative components  $F_{l^e,t}^{e+}$ ,  $F_{l^e,t}^{e-}$  as well as the power injection at each bus. A linear coefficient  $\delta_{l^e}^e$  for the branch losses is introduced together with the matrices  $\mathbf{M}_{BI}$  and  $\mathbf{M}_{BLE}^e$  that represent the grid topology -  $M_{bi} = 1$  if unit  $i$  is connected to bus  $b$ ;  $M_{bl^e}^e = 1$  if line  $l^e$  starts/ends at bus  $b$ . Finally, line power flow is computed according to (15). As in the method developed in [19] the losses within a line are equally distributed at the start and end buses as additional loads. The power balance constraint is modified following (16) to consider the balance at each bus  $b$  for every time step  $t$ . Finally, constraints (17) ensure that the line power flow remains below the specified limit  $F_{l^e}^{e-M}$ .

$$F_{l^e,t}^{e+} - F_{l^e,t}^{e-} = \sum_{b \in B} SF_{l^e b} \times \left( \sum_{i \in I} M_{bi} \times P_{i,t}^e - P_{b,t}^{L-e} + M_{bl^e}^e \times \frac{\delta_{l^e}^e}{2} \times (F_{l^e,t}^{e+} + F_{l^e,t}^{e-}) \right) \quad (15)$$

$$\sum_{i \in I} M_{bi} \times P_{i,t}^e + \sum_{l^e \in L^E} M_{bl^e}^e \times \frac{\delta_{l^e}^e}{2} \times (F_{l^e,t}^{e+} + F_{l^e,t}^{e-}) = P_{b,t}^{L-e} \quad (16)$$

$$\begin{cases} F_{l^e,t}^{e+}, F_{l^e,t}^{e-} \geq 0 \\ -F_{l^e}^{e-M} \leq F_{l^e,t}^{e+} - F_{l^e,t}^{e-} \leq F_{l^e}^{e-M} \end{cases} \quad (17)$$

#### 2) Thermal Grid Model

The thermal grid displays two main differences compared to the power system. Firstly, the steam flows  $F_{l^h,t}^h$  in the pipe  $l^h$  are strictly unidirectional because of the irreversibility of turbomachinery [20]. Secondly, those steam flows can only take values below a predefined capacity  $F_{l^h}^{h-des}$  within a certain range  $\theta$  (typically 25 %) [21] ((18)). In order to ensure the convergence of the scheduling problem, controllable damp loads  $P_{b,t}^{dp}$  and boilers  $P_{b,t}^{bl}$  should be considered at each bus. In particular, they allow more flexibility if the units' operating conditions and the heat flow limits do not allow the supply of loads  $P_{b,t}^{bl}$  or if there is a local excess of heat generation. Finally the heat balance at each bus is expressed using (19) with  $\mathbf{M}_{BLH}^{h+}$  and  $\mathbf{M}_{BLH}^{h-}$   $B \times L^H$  matrixes that map the heat network -  $M_{bl^h}^{h+} = 1$  if line  $l^h$  ending at bus  $b$  and  $M_{bl^h}^{h-} = 1$  if  $l^h$  starting from bus  $b$ . The equation also considers linear loss coefficients  $\delta_{l^h}^h$  that depends on the pipe length.

$$\left( 1 - \frac{\theta}{100} \right) \times F_{l^h}^{h-des} \leq F_{l^h,t}^h \leq F_{l^h}^{h-des} \quad (18)$$

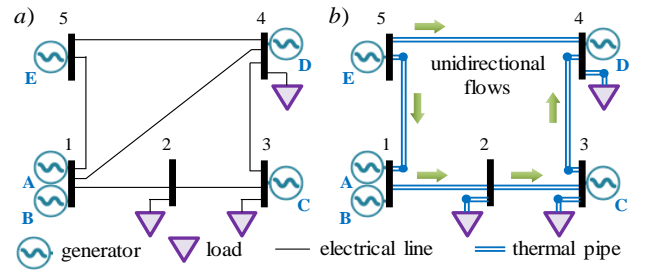


Fig. 9: 5 bus system – a) electrical network – b) thermal network

TABLE IV  
Steam pipes parameters

Pipe	1-2	2-3	3-4	4-5	1-5
$F_{l^h}^{h-des}$ (MW)	400	200	100	200	300
$\delta_{l^h}^h$ (%)	3.9	1.5	4.2	4.2	0.9

$$\begin{aligned} \sum_{i \in I} M_{bi} \times P_{i,t}^h + \sum_{l^h \in L^H} M_{bl^h}^{h-} \times (1 - \delta_{l^h}^h) \times F_{l^h,t}^h - M_{bl^h}^{h+} \times F_{l^h,t}^h = \dots \\ \dots P_{b,t}^{dp} + P_{b,t}^{L-e} - P_{b,t}^{bl} \end{aligned} \quad (19)$$

### B. Obtained Results.

#### 1) 5-bus Test Case

The power/heat dispatch problem with grid constraints is implemented for the 5-bus system displayed in Fig. 9. Parameters for power lines and maximum outputs of the generators are derived from [22] with technical parameters corresponding to the CCGT units in Jurong Island (five units A, B, C, D and E). A thermal network is designed with the topology depicted in Fig. 9b with specified directions for the steam flows. The pipes capacities as well as the heat loss coefficients are given in Table IV. Three daily profiles are considered for the electrical loads at buses 2,3 and 4. The heat profiles are assumed to follow the same patterns, and different levels of power/heat demands can be investigated. First, an optimal scheduling is considered with a heat load equals to 150 % of the power demand profile and the boilers specific CO<sub>2</sub> emission is set at 500 kg/MWh. A preliminary test is performed while running the optimal dispatch with all the power/heat ratios set to 1 for every unit (S1) and it corresponds to 9639 tons of CO<sub>2</sub> emitted for the representative day. Then the hybrid Greedy/MILP dispatch (SGD) presented in the previous section is applied to minimize the CO<sub>2</sub> emissions with adjusted  $r_i^{ref}$  (integers in {1,11} for power/heat ratio in [0,1]). Emissions are significantly reduced to 8123 tons (16 % reduction) with the CCGT units generating more heat than in S1.

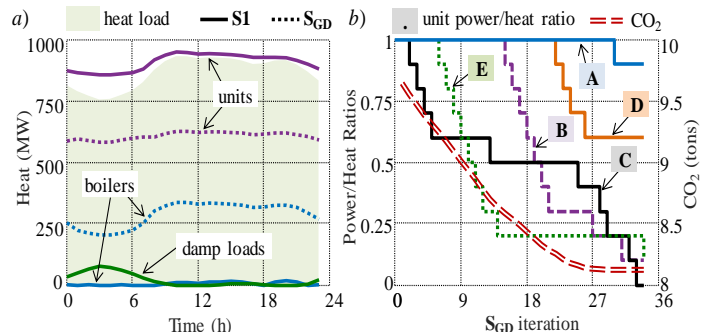


Fig. 10: Obtained results – a) heat load supply – b) greedy search method

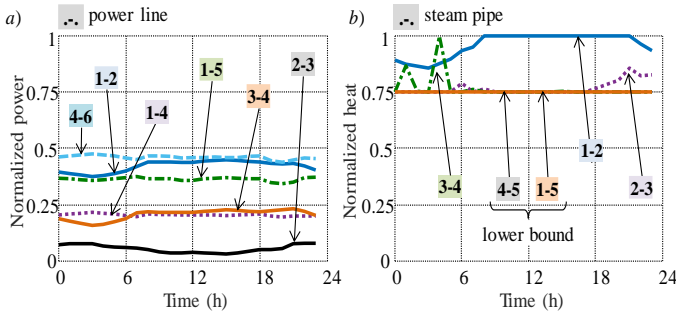


Fig. 11: Branch flows – a) power lines – b) steam pipes

As displayed in Fig. 10a the increase of the waste heat generation in  $S_{GD}$  allows extensive use of the boilers to be avoided, resulting in reduced CO<sub>2</sub> emissions. For low heat load levels, the CCGT heat production is even greater than the demand. The use of damp loads is then required, which is not necessary in  $S_1$ . During peak load, hours the heat generation remains slightly greater than the load as it feeds the system heat losses (Fig. 10a). The convergence of the greedy method is reached after 45 min of computation with 34 iterations, which corresponds to 169 evaluations of the objective function (i.e. runs of the MILP dispatch with constant ratios). The optimal solution returned displays relatively low values for the power/heat ratios compared to the previous case study with two units (unit A: 0.9, unit B: 0.1, unit C: 0, unit D: 0.6 and unit E: 0.1). That is explained by the electrical power load being significantly lower than the installed capacity: the peak load is 620 MW for 1.2 GW of total capacity. There is no problem for the CCGT units to operate at lower power/heat ratios while supplying the electrical demand. Thus those ratios decrease along the iterations of the greedy search method as well as the CO<sub>2</sub> emissions until no improvement is possible (Fig. 10b). Fig. 11 displays the line flows normalized by the maximum capacities. The powers within the electrical lines are not important (below 50 % of load) as the electrical demand level is low compared to the system capacity (Fig. 11a). Regarding the steam pipes, the lower bound for the heat flows appears to be a binding constraint (Fig. 11b). Indeed, except for line 1-2 all the flows remain close to the minimum value which then requires the generation of additional heat (either with the boilers of the CCGT units).

An additional set of simulations is performed, varying the heat load level (in % of power demand) as well as relaxing the steam flow constraint with greater values for  $\theta$  (which is not realistic). The CO<sub>2</sub> emissions are computed for the two scenarios  $S_1$  and  $S_{GD}$  and the obtained results are compiled in Table V. As already observed in Section IV the improvements provided by an optimal dispatch compared to  $S_1$  tend to increase with greater levels of heat demand. The relaxation of the thermal flow constraints also allows greater CO<sub>2</sub> reductions in all cases. The obtained results confirm that the constraint is a binding limit for all the considered load levels and while applying both dispatch  $S_1$  and  $S_{GD}$ . Thus the design capacity of the pipe should be appropriately determined in the planning phase when dealing with cogeneration problems [5]-[7]. On the one hand, undersized pipes would limit the use of the heat generation capacity of the units. On the other, oversized lines might require additional boilers to operate under low load condition to maintain a minimal flow in the branches.

TABLE V  
Impact of steam flows limits

Heat load level	50 %		100 %		150 %	
	$S_1$	$S_{GD}$	$S_1$	$S_{GD}$	$S_1$	$S_{GD}$
$\theta = 25 \%$	6741	6235	7595	6999	9639	8123
$\theta = 50 \%$	5425	5425	6821	6484	9539	7647
$\theta = 75 \%$	5111	5111	6207	6187	9474	7617
$\theta = 100 \%$	5111	5111	6169	6122	9448	7610

## 2) Jurong Island Model

Final set of simulations refers to the model of Jurong Island. The power grid is represented by a 208 buses, 219 branch model and the thermal network displays 14 nodes and 14 steam pipes. The distinction is made between purely electrical customers and nodes with both thermal and electrical loads (Fig. 12a). Heavy customers (e.g. oil refineries) are assumed to get their own steam supply while the other thermal loads are aggregated into mutualized heating districts (Fig. 12b). Losses are computed based on the cable/pipe characteristics and the estimated distances between the buses. Simulations are run for  $A^{bl} = 500$  kg/MWh and  $\theta = 25 \%$ . Three levels of heat demand are investigated (i.e. low **L**, medium **M** and high **H**). Similar to Section IV,  $S_1$  corresponds to an optimal dispatch with all the power/heat ratios set to 1 for every unit and  $S_{GD}$  to the application of the hybrid Greedy/MILP dispatch. Results obtained in the various cases are displayed in Table VI.

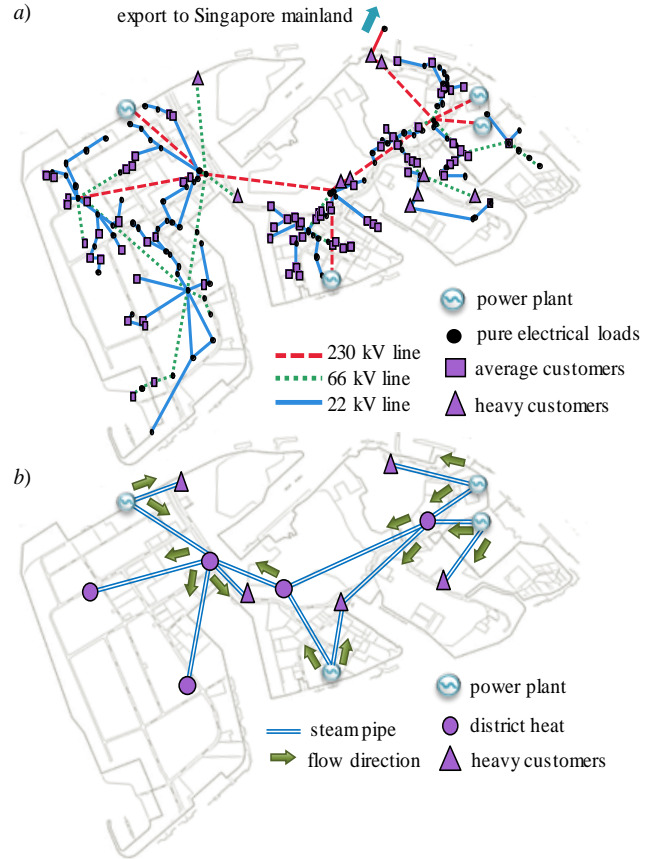


Fig. 12: Jurong Island – a) power grid – b) thermal network

TABLE VI  
CO<sub>2</sub> emissions for different heat load levels

Heat load level	<b>S<sub>I</sub></b>	<b>S<sub>GD</sub></b>
<b>L</b>	33385	32201
<b>M</b>	41757	39415
<b>H</b>	56558	53801

The computational time to run **S<sub>GD</sub>** remains significant even with the use of the greedy search from 3 h for the case **L** to more than 5 hours for case **H**, for the representative day. As already observed the improvements are more significant for higher heat load levels. Following the remarks of the previous subsection, better results could be obtained by investigating different steam pipe capacity configurations. Additionally, not all the units might have to be considered in the power/heat dispatch. Indeed, for the three investigated load levels, only three to four CCGT actively participate in the steam supply with optimal power/heat ratios lower than 1.

## VI. CONCLUSIONS

This paper successfully implemented a CCGT model for power and heat cogeneration as well as an efficient power dispatch strategy based on the minimization of CO<sub>2</sub> emissions. The obtained results show significant improvements compared to a case where cogeneration units are not controllable (i.e. priority given to electrical output). Those improvements become greater when higher heat load levels or dirtier additional boilers are considered. The observations also showed the necessity to appropriately size the steam pipes as lower bounds for heat flows are binding constraints in most cases. Further work may investigate design strategies. Also, other cost components should be included in the dispatch objective, in addition the CO<sub>2</sub> emissions that have been considered so far.

## VII. ACKNOWLEDGMENT

This work was supported by the Singapore National Research Foundation (NRF) under its Campus for Research Excellence and Technological Enterprise (CREATE) programme, specially the Cambridge Centre for Advanced Research in Energy Efficiency in Singapore (CARES).

## VIII. REFERENCES

- [1] R. Hashemi, "A developed offline model for optimal operation of combined heating and cooling and power systems", *IEEE Transactions on Energy Conversion*, vol 24, no 1, pp. 222-229, 2009.
- [2] M. Kia, M. S. Nazar, M. S. Sepasian, "Optimal day ahead scheduling of combined heat and power units with electrical and thermal storage considering security constraint of power system", *Energy*, vol 120, pp. 241-252, 2017.
- [3] C. Shao, Y. Ding, J. Wang, Y. Song, "Modeling and Integration of Flexible Demand in Heat and Electricity Integrated Energy System", *IEEE Transactions on Sustainable Energy*, vol 9, no 1, pp. 361-370, 2018.
- [4] A. H. Azit, K. M. Nor, "Optimal sizing for a gas-fired grid-connected cogeneration system planning", *IEEE Transactions on Energy Conversion*, vol 24, no 4, pp. 950-958, 2009.
- [5] Z. Li, W. Wu, J. Wang, B. Zhang, T. Zheng, "Transmission-Constrained Unit Commitment Considering Combined Electricity and District Heating Networks", *IEEE Transactions on Sustainable Energy*, vol 7, no 2, pp. 480-492, 2016.
- [6] J. Ye, R. Yuan, "Integrated natural gas, heat, and power dispatch considering wind power and power-to-gas", *Sustainability*, vol. 9, no 602, pp. 1-16, 2017.

- [7] X. Zhang, G. G. Karady, S. T. Ariaratnam, "Optimal Allocation of CHP-Based Distributed Generation on Urban Energy Distribution Networks", *IEEE Transactions on Sustainable Energy*, vol 5, no 1, pp. 246-253, 2014.
- [8] R. Rigo-Mariani, K. V. Ling, J. Maciejowski, "A generic method to model CO<sub>2</sub> emission performances of combined-cycle power plants for environmental unit commitment", *Energy Technology*, vol 6, no 1, pp.72-83, 2018.
- [9] C. Zhang, A. Romagnoli, L. Zhou, and M. Kraft, "Knowledge management of eco-industrial park for efficient energy utilization through ontology-based approach," *Applied Energy*, vol 204, , pp. 1412-1421 2017.
- [10] M. P. Boyce, "Handbook for cogeneration and combined cycle power plants", 2nd ed., *ASME Press*, 2010.
- [11] T. S. Kim, "Comparative analysis on the part load performance of combined cycle plants considering design performance and power control strategy", *Energy*, 2004, vol 29, pp.71 –85, 2004.
- [12] C. D'Ambrosio, A. Lodi, S. Martello, "Piecewise linear approximation of functions of two variables in MILP models", *Operations Research Letters*, vol 38, pp 39-46, 2010.
- [13] M. Carrión, J. M. Arroyo, "A computationally efficient mixed-integer linear formulation for the thermal unit commitment problem", *IEEE Trans. On Power Systems*, vol 21, no 3, pp 1371-1378, 2006.
- [14] Y. Zhang, J. McKechnie, D. Cormier, R. Lyng, W. Mabee, A. Ogino, et al., "Life Cycle Emissions and Cost of Producing Electricity from Coal, Natural Gas, and Wood Pellets in Ontario, Canada," *Environmental Science & Technology*, vol. 44, pp. 538-544, 2010.
- [15] S. Eggleston, L. Buendia, K. Miwa, T. Ngara, K. Tanabe, "2006 IPCC guidelines for national greenhouse gas inventories", Insitute for Global Environmental Strategies, Japan, 2006. [Online] <https://www.ipcc-nggip.iges.or.jp/public/2006gl>
- [16] K. Van den Bergh, K. Bruninx, E. Delarue, W. D'haeseleer, "A Mixed-Integer Linear Formulation of the Unit Commitment Problem", KU Leuven, TME working paper, 2014. [Online] Available: [https://www.mech.kuleuven.be/en/tme/research/energy\\_environment/Pd f/wpen2014-07.pdf](https://www.mech.kuleuven.be/en/tme/research/energy_environment/Pd f/wpen2014-07.pdf)
- [17] J. Lofberg, "YALMIP: a toolbox for modelling and optimization in MATLAB", IEEE International Symposium on Computer Aided Control Systems Design, New-Orleans, USA, pp. 282-289, 2004.
- [18] C. Bardulescu, S. Kilyeni, G. Vuc, B. Lustrea, R. E. Precup, S. Preitl, "Software tool for power transfer distribution factor (PTDF) computing within the power systems", IEEE EUROCON, pp. 517-524, St.-Petersburg, Russia, 2009.
- [19] F. Li, "Fully reference-independent LMP decomposition using reference-independent loss factors", *Electric Power System Research*, vol 81, pp 1995-2004, 2011.
- [20] H. Lund, S. Werner, R. Wiltshire, S. Svendsen, J. E. Thorsen, F. Hvelplund, et al., "4th Generation District Heating (4GDH): Integrating smart thermal grids into future sustainable energy systems," *Energy*, vol. 68, pp. 1-11, 2014.
- [21] H. Wang, H. Wang, T. Zhu, and W. Deng, "A novel model for steam transportation considering drainage loss in pipeline networks", *Applied energy*, vol. 188, pp. 178-189, 2017.
- [22] F. Li, R. Bo, "Small test systems for power system economic studies", Power and Energy Society General Meeting, Providence, USA, 2010.